Trop J Nat Prod Res, November 2025; 9(11): 5529 - 5536 **ISSN 2616-0684 (Print)**
**ISSN 2616-0692 (Electronic)**

# Tropical Journal of Natural Product Research

Available online at https://www.tjnpr.org

*Original Research Article*

# Design, Synthesis, and *In Silico* Investigation of A Polyheterocyclic Scaffold as A Potential Dual CDK9/Caspase-6 Inhibitor

Delfaa S. Gassed[1], Murad G. Munahi[2], Hawraa A. Mazyed[3]*, Wijdan A. Eneamah[4], Noor A. Almosawi[5]

[1] *Chemistry Department/College of Science, Basrah University, Iraq*
[2] *Department of Biology/College of Science/Al-Muthanna University, Iraq*
[3] *Department of Chemistry/College of Science/Al-Muthanna University, Iraq*
[4] *Department of Pharmaceutical Chemistry. College of Pharmacy, Al-Ayen Iraqi University, Iraq*
[5] *Department of Pharmaceutical Chemistry, College of Pharmacy, Basrah University, Iraq*

ARTICLE INFO

*Article history:*
Received 02 September 2025
Revised 22 October 2025
Accepted 24 October 2025
Published online 01 December 2025



ABSTRACT

Developing novel therapeutic agents remains a major focus in medicinal chemistry, particularly for cancer and neuroinflammatory disorders. A novel polyheterocyclic compound was synthesised and structurally characterized by FT-IR, $^{1}$H NMR, and $^{13}$C NMR spectra. To assess its therapeutic potential, an integrated computational approach was conducted, including ligand-based virtual screening, molecular docking, and ADMET predictions. Among five predicted targets, CDK9–Cyclin T1 and Caspase-6 exhibited the most favorable binding profiles, with docking scores of −8.78 kcal/mol and −8.52 kcal/mol, respectively. The compound exhibited key interactions within the active sites of CDK9 and Caspase-6, resembling those of the reference inhibitors Alvocidib and Emricasan. Notably, key interactions with CDK9 involved Glu107 and Asp167, indicating potential for transcriptional inhibition via targets like MYC and MCL-1. Furthermore, the ADME predictions report favourable pharmacokinetic properties, supporting the compound's candidacy for future biological evaluation as an anticancer and a neuro-antiinflammatory agent.

***Keywords:*** Heterocyclic compounds, 1,2,3-Triazole, Furan ring, molecular docking, cyclin-dependent kinase 9 / Cyclin T1, Cysteine-aspartic protease 6.

## Introduction

The chemistry of heterocyclic compounds is a vital field in modern organic chemistry. Heterocyclic compounds are widely occurring in living nature and play a key role in the metabolism of living organisms, especially those that contain heteroatoms such as nitrogen, oxygen, and sulfur in their structure.[1] This is particularly evident in five-membered heterocyclic compounds containing more than one ring in their structure, as their structural diversity often leads to significant pharmacological activities, exemplified by compounds such as furan, pyrrole, and thiophene.[2] Notably, hybrid molecules incorporating these rings have demonstrated significant potential in medicinal chemistry, serving as lead compounds for anticancer drug development due to their ability to effectively inhibit cancer cell growth and induce apoptosis, making them promising candidates for cancer therapy.[3] Also, these compounds demonstrate antimicrobial activity, which is crucial for developing new antibiotics and antifungals by inhibiting microbial growth.[4] Their neuroprotective effects also contribute to their therapeutic applications, particularly in treating neurodegenerative diseases by promoting neuronal survival.[5] Furthermore, polyheterocyclic compounds show cardiovascular activity, modulating cardiovascular function and potentially alleviating symptoms associated with cardiovascular diseases,[6] while also possessing antioxidant properties.[7] cyclin-dependent kinase 9 (CDK9)/Cyclin T1 is considered one of the major regulators of RNA polymerase II-mediated productive transcription of critical genes in any cell.

*Corresponding author. E mail: Hawraa.abdulkadhim@mu.edu.iq
Tel.: +9647818914611

**Citation:** Gassed DS, Munahi MG, Mazyed HA, Eneamah WA, Almosawi NA. Design, Synthesis, and *In Silico* Investigation of A Polyheterocyclic Scaffold as A Potential Dual CDK9/Caspase-6 Inhibitor. Trop J Nat Prod Res. 2025; 9(11): 5529 – 5536 https://doi.org/10.26538/tjnpr/v9i11.36

Official Journal of Natural Product Research Group, Faculty of Pharmacy, University of Benin, Benin City, Nigeria

The activity of CDK9 is significantly upregulated in a wide variety of cancer entities to aid in the overexpression of genes responsible for the regulation of functions that are beneficial to the cancer cells, like proliferation, survival, cell cycle regulation, DNA damage repair, and metastasis.[8] Enhanced CDK9 activity, therefore, leads to poorer prognosis in many cancer types, offering the rationale to target it using small-molecule inhibitors. The inhibition of CDK9's activity offers an effective anti-cancer therapeutic strategy.[9] Similarly, Caspase-6 is widely expressed in the brain and peripheral tissues, and, in addition to being involved in apoptosis, represents a vital target in neurodegenerative drug discovery.[10] Here, in this study, we have synthesised a heterocyclic compound bearing five-membered multiple rings, such as furan and pyrrole. This compound's unique structural combination, not previously reported to our knowledge, creates a versatile platform for drug design due to its structural and electronic diversity, potentially enabling interactions with multiple targets in complex diseases.

The ability of such multifunctional heterocycles to modulate both CDK9 and caspase-6 highlights their potential as dual-acting therapeutic agents in cancer and neurodegeneration.

## Materials and Methods

*Materials*

All solvents and starting materials were purchased from commercially available sources and directly used without further purification: Acetylacetone (≥99% purity, analytical grade, Sigma-Aldrich, USA), Ethanol (99.9% purity, HPLC grade, Sigma-Aldrich, USA), Potassium hydroxide (≥85% purity, pellets, analytical grade, BDH Chemicals, UK), Hydrochloric acid (37% purity, reagent grade, Scharlau, Spain), Methanol (≥99.8% purity, HPLC grade, Sigma-Aldrich, USA). All instruments and equipment used in this study were operated in the Central Laboratories of the University of Basrah and the University of Al-Muthanna, Iraq. The FT-IR spectra were recorded on a Shimadzu

ISSN 2616-0684 (Print)
ISSN 2616-0692 (Electronic)

FT-IR 8400 spectrometer in KBr discs. NMR spectra were acquired using an Inova NMR spectrometer (500 MHz for $^{1}$H NMR spectra and 125 MHz for $^{13}$C NMR spectra), and the chemical shifts (σ) were given in ppm.

Synthesis of compounds 1-3: Compounds 1-3 were prepared previously as described in the literature.[11, 12, 13]

Synthesis of compound 4: A mixture of chalcone derivative 3 (5 mmol) and acetylacetone (5 mmol) in ethanol (60%, 25 mL) containing aqueous potassium hydroxide solution (5 mL, 40%) was refluxed for 10 hr., and the reaction mixture was evaporated to half by using the rotary evaporator and then acidified with 1:1 HCl and $H_2O$. The solid precipitate was filtered under vacuum, washed with ether, and recrystallised from methanol to give the target product (4). Yield (2.10 g, 95.67%), brown powder, m.p. 355-357 °C. FT-IR (KBr disc, $cm^{-1}$): 3454.62 (OH, sulfonyl), 3066.92 (Ar-H), 2947.33 (sp3 aliphatic, C-H), 1716.70 and 1683.91 (C=O), 1643.41 (C=C), 1600.97 (C=C), 1554.68 (Ar, C=C), 1504.53 (-N=N), 1124.75 (C-O). $^{1}$H-NMR (400 MHz, DMSO-d6): δ(ppm) = 2.27 (s, 3H, C<u>H</u>$_3$-C=O), 2.56 (s, 3H, C<u>H</u>$_3$ of triazole ring), 5.63 (s, 1H, O=C-C<u>H</u>-C=O), 7.54-7.61 and 9.00 (s, 3H, -C<u>H</u> of furan ring), 8.14 (s, 1H, -C<u>H</u>-C=O), 8.57 (s, 1H, CH), 8.79-8.82 (d, 4H, Ar-H). $^{13}$C-NMR (101 MHz, DMSO-d6): δ(ppm) = 9.51, 27.31, 72.78, 118.60, 123.74, 123.73, 127.12, 127.48, 127.67, 127.99, 132.39, 137.21, 137.83, 138.8., 139.00, 144.68, 156.02,184.77, 192.79.

*In silico* study

*Ligand-Based Virtual Screening*

A suitable strategy called ligand-based virtual screening was used to predict the potential targets of the synthesised compound 4; the Swiss Target server (http://www.swisstargetprediction.ch/ ) was used to predict the targets.[14] Compound 4 was subjected to virtual screening against more than 3000 receptors found in humans, and the server provided a ranked list of potential targets based on their predicted probability. The top five candidate targets (casein kinase II alpha, CDK9/cyclin T1, caspase-3, caspase-6, and caspase-7) were highlighted and selected for molecular docking.

*Protein selection*

The proteins were obtained from the RCSB Protein Data Bank (https://www.rcsb.org/). All of the undesired organic molecules, ions, and water molecules were removed using AutoDock Tools (ADT) release 1.5.6[15]. Polar hydrogen atoms were added, and partial charges were calculated using the Gasteiger charge method to the protein using ADT.[16] PDB codes, active sites, and grid dimensions are illustrated in Table 1.

**Table 1:** Docking preparation parameters for the selected targets.

| Target | Pdb code | Active residues | Grid size (x, y, z) | Grid center (x, y, z) | Ref. |
|---|---|---|---|---|---|
| Casein kinase II alpha | 6HOR | Leu45, Val53, Val66, Lys68, Glu81, Ile95, Phe113, Val116, Met163, Ile174, Asp175, Try176 | 42,60, 40 | -21.943, 11.495, -13.154 | 20 |
| CDK9/cyclin T1 | 8K5R | Phe103, Phe105, Cys106, Glu107, Asp167, Phe168 | 64, 40, 40 | 53.013, -13.86, -10.588 | 21 |
| Caspase-3 | 3H0E | Thr62, Arg64, His121, Glu123, Gln161, Cys163, Tyr204, Ser205, Trp206, Arg207, Asn208, Ser209, Phe250, Phe256 | 50, 62, 62 | 26.066, 54.722, 11.231 | 22 |
| Caspase-6 | 3OD5 | Arg 64, His121, Gly122, Gln 161, Cys163,His168, Tyr217, His219, Arg220, Glu221, Trp227, Val261 | 54, 48, 58 | 29.716, 5.521, 25.146 | 23 |
| Caspase-7 | 1F1J | Gly85, Arg87, His144, Gly145, Gln184, Cys186, Tyr230, Ser231, Trp232, Arg233, Pro235, Gln276, Phe282 | 58, 50, 52 | 37.205, 25.874, -2.847 | 24 |

*Molecular docking*

Molecular docking using Autodock vina v.1.1.2,[17] was performed for compound 4 against the potential five targets, and then the targets with good results were selected for further analysis. The structure of compound 4 was drawn using ChemDraw Ultra 12.0 software. The 3D sketched ligand 4 was converted to PDBQT format using Open Babel v. 2.0. The best conformations were regarded as having the lowest binding energy. The most favourable conformations according to binding energy were selected. Discovery Studio Visualiser (v.4.5) was employed to visualise the intermolecular interactions between the receptors and ligand.[18]

*ADME prediction*

The pharmacokinetic profiles of the synthesised compound (Compound 4) were evaluated using the ADMETlab 2.0 webserver (https://admetmesh.scbdd.com). This platform is composed of a wide range of machine learning models to predict absorption, distribution, metabolism, and excretion (ADME) properties based on the compound's SMILES representation. The analysis included key parameters such as physicochemical properties, oral bioavailability, human intestinal absorption, blood–brain barrier permeability, plasma protein binding, cytochrome P450 interactions, and clearance.[19] All predictions were performed using default settings and evaluated for compliance with standard drug-likeness and safety criteria.

ISSN 2616-0684 (Print)
ISSN 2616-0692 (Electronic)

## Results and Discussion

The synthesis of Compound 4 was performed according to the synthetic route outlined in Scheme 1. Mainly, the cycloaddition reaction of compound 1 with the commercially available acetylacetone in the presence of triethylamine under moderate temperature leads to the construction of a 1,2,3-triazole ring to give 1,2,3-triazole derivative 2. Followed by a condensation reaction with a series of the commercially available aromatic aldehydes under Claisen–Schmidt condensation conditions to give the corresponding chalcone 3. This route involved the reaction of the synthesised compound 3 with commercially available acetylacetone in the presence of an aqueous potassium hydroxide solution under reflux for 10 hours. The workup revealed that the reaction proceeded smoothly, yielding the target compound 4 in good yield with high purity. The structure of compound 4 was confirmed by FT-IR, $^{1}$H-NMR, and $^{13}$C-NMR spectra. The FT-IR spectra of compound 4 revealed a significant discovery; the emergence of new absorption bands at 1714.7 $cm^{-1}$ and 1683.9 $cm^{-1}$. These bands can be attributed to the incorporation of carbonyl groups (-C=O) and the attachment of carbonyl groups (-$COCH_3$) to the cyclohexane ring, respectively. Their appearance is directly linked to the disappearance of the absorbance band characteristic of the chalcone structure. In addition, the $^{1}$H-NMR spectra exhibited two singlet peaks at 2.28 and 5.01 ppm, which refer to protons of the ketonic methyl group (-$COCH_3$) and (O=C-CH-C=O), respectively. As well, two singlet peaks appeared at 6.55 ppm and 7.03 ppm, which belong to (-CH=C) and (=CH-CO) of the cyclohexane ring, respectively. Additionally, the protons of aromatic rings and the methyl group attached to the triazole ring system appeared at their expected chemical shifts with the correct integrals. All these results indicated that the cyclohexa-2,4-dienone ring had been formed. Moreover, the data obtained from $^{13}$CNMR spectra were in agreement with the findings of FT-IR and $^{1}$H-NMR spectroscopy.

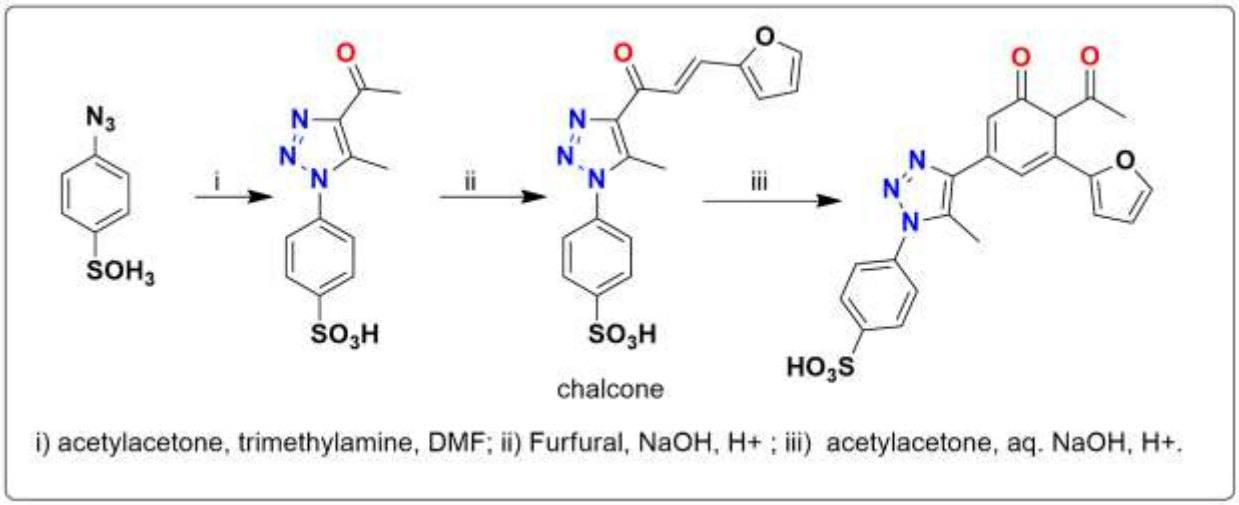


**Scheme 1:** Synthesis pathway of compound 4

*Virtual Screening and Molecular Docking*

In general, molecular docking is one of the most powerful techniques used in drug discovery; however, in traditional docking strategies, targets are often selected somewhat randomly based on the anticipated ability of synthesised compounds to inhibit them. To avoid this random selection of vital enzymes involved in key biological pathways, we first employed a powerful approach known as ligand-based virtual screening to predict the potential targets of our compounds. The present study employed an integrated *in silico* workflow to identify potential human targets for compound 4, followed by docking-based validation of binding affinity and active site engagement. The Swiss Target Prediction web server was used to predict the target of the synthesised compound (4), this server explored the potential targets for the input molecule, where it screened the molecule against thousands of enzymes. The server provided a ranked list of potential targets based on their predicted probability. The top five candidate targets (Casein kinase II alpha, CDK9/cyclin T1, Caspase-3, Caspase-6, and Caspase-7) were highlighted (Table 1); these targets were subjected to molecular docking for further validation. From the initial five predicted targets, CDK9–Cyclin T1 and Caspase 6 emerged as the most promising, demonstrating both favourable binding energies compared to the control drugs and proper orientation within the respective active sites (Tables 1 and 2 and Figures 2 and 3). This selective retention highlights the value of coupling ligand-based virtual screening with structure-based docking as a dual-filter strategy to eliminate false positives arising from the random selection of targets.

Although casein kinase II α, caspase 3 and caspase 7 showed good binding scores comparable to the standard drugs, visual inspection revealed that the favorable energy poses lay either at the protein surface or in shallow grooves that do not overlap the defined active sites (Table 1). Due to such orientations being unlikely to be translated into active inhibition, these three proteins were excluded from further analysis despite their attractive ΔG values. This observation emphasises the importance of not relying solely on ΔG values in virtual screening approaches, as a ligand may exhibit good binding energies while primarily interacting with inactive residues, particularly located at the protein surface or solvent-exposed grooves. Thus, spatial orientations within functional pockets are a critical determinant of enzyme inhibition.

The visualisation of CDK9–Cyclin T1/ compound 4 revealed that Compound 4 nests deeply in the ATP-binding cleft, mimicking the anchoring geometry of the reference inhibitor Alvocidib and gaining additional stabilisation (ΔG = -8.78 kcal/mol vs -8.18 kcal/mol for Alvocidib). The ligand engages all six catalytic residues (Phe103, Phe105, Cys106, Glu107, Asp167, Phe168) through a complementary variety of interactions, as illustrated by Table 3. Together, these contacts fully occupy the ATP site, leaving little void volume and preventing water intrusion. The superposition in Figure 1 shows a weak overlap of compound 4 with Alvocidib; however, the extra H-bond network (three vs two) and a broader hydrophobic footprint rationalise its slightly superior docking score.

ISSN 2616-0684 (Print)
ISSN 2616-0692 (Electronic)

**Table 2:** Molecular docking results of Compound 4 against the top five potential targets (scores represent the averages of five replicates).

| Target | Docking score (compound 4) | Docking score (Control) |
|---|---|---|
| Casein kinase II alpha | -8.72±0.11 | -10.06±0.08 |
| CDK9/cyclin T1 | -8.78±0.38 | -8.18±0.04 |
| Caspase-3 | -9.38±0.07 | -8.9±0.08 |
| Caspase-6 | -8.52±0.04 | -8.18± 0.33 |
| Caspase-7 | -9.48±0.04 | -9.34±0.31 |

**Table 3:** Key ligand–residue interactions and their structural contributions within the binding pocket of CDK9–Cyclin T1.

| Residue | Interaction type | Structural contribution |
|---|---|---|
| Phe103, Phe105, | π–π stacking with the triazole-substituted phenyl ring | Forms an aromatic "sandwich" that locks the ligand along the hydrophobic wall of the pocket |
| Cys106 | van-der-Waals | Helps to orient the carbonyl oxygen towards the hinge region |
| Asp109 | H-bond | Anchors the ligand at the hinge, a hallmark interaction for potent CDK inhibitors |
| Asp167 | H-bond | One of three H-bonds; critical for inhibition and selectivity |
| Phe168 | π -donor hydrogen bond | likely stabilizes the position and orientation of the triazole ring, enhancing both binding affinity and specificity |

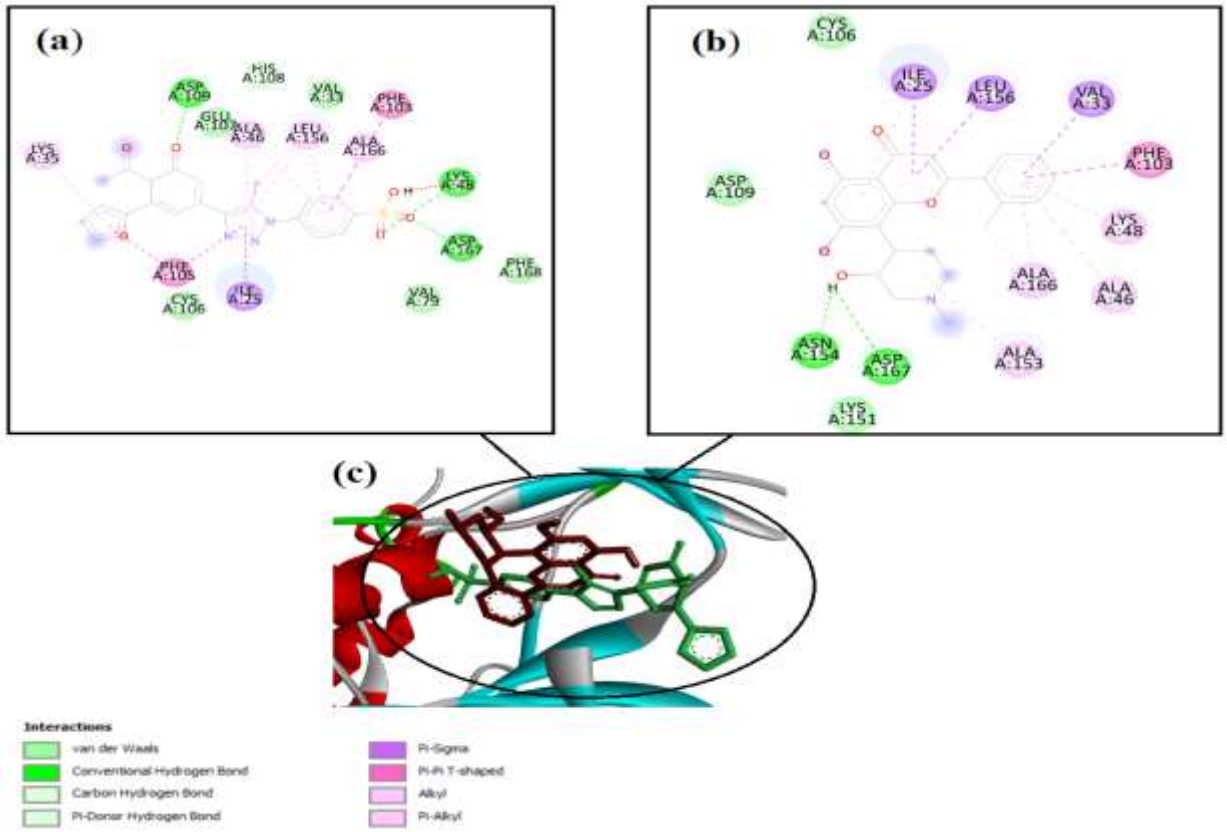


**Figure 1:** Interaction diagrams showing (a) compound 4 in complex with CDK9-cyclin T1, (b) the standard drug Alvocidib in complex with CDK9-cyclin T1, and (c) superpositioning of compound 4 (Green) and Alvocidib (Red).

The active site residues of Caspase-6, including Arg64, His121, Gly122, Gln161, Cys163, His168, Tyr217, His219, Arg220, Glu221, Trp227, and Val261, played a crucial role in ligand recognition and stabilization. Compound 4 demonstrated a strong binding through multiple interactions, notably π–π stacking with Val261, van der Waals with Trp227, hydrogen bonding with His168, Asp262, and Phe263, and π–cation interaction with His219. These interactions contributed to the stabilization of the ligand within the hydrophobic pocket, particularly between aromatic residues such as Tyr217 and Trp227. Moreover, compound 4 showed deeper anchoring into the active site cleft and maintained contact with catalytically relevant residues, particularly His219 and Glu221, indicating a potentially stronger and more specific binding profile compared to the standard Emricasan. The visualised superpositioning (Figure 2C) further confirmed that compound 4 is favorably oriented within the active pocket, thereby positioned compatibly with the key binding hotspots essential for Caspase-6 inhibition.

ISSN 2616-0684 (Print)
ISSN 2616-0692 (Electronic)

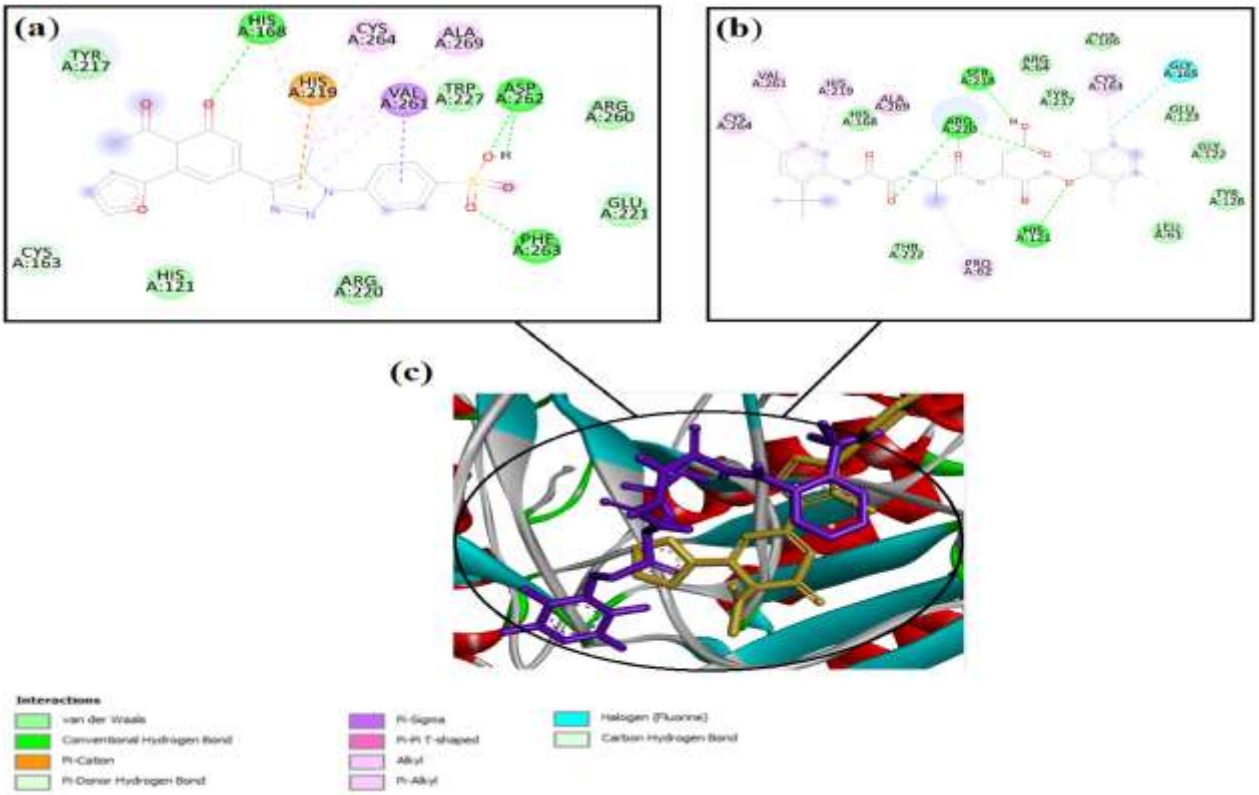


**Figure 2:** Interaction diagrams showing (a) compound 4 in complex with Caspase 6, (b) the experimental drug Emricasan in complex with Caspase 6, and (c) superpositioning of compound 4 (Yellow) and Emricasan (Purple).

Our docking analysis found that compound 4 binds deeply in the caspase 6 catalytic pocket while showing no effective poses in caspases 7 or 9, highlighting accurate family-member selectivity. Such isoform specificity is rarely achieved: even the most advanced tested compounds rely on covalent capture with the unique Cys264 side chain to recognise caspase 6 from its relatives.[25] Therefore, compound 4 provides a non-covalent targeting that may reduce off-target apoptosis and associated toxicity.

This dual-target potential modulation of both transcription and apoptosis pathways may lead to new opportunities for a potent therapeutic strategy, especially in cancer or inflammatory settings where CDK9 and caspases are co-regulated. A single drug with dual activity offers several advantages over fixed-dose combinations, including simplified pharmacokinetics, reduced pill burden, intrinsically synchronised target engagement, and a lower probability of parallel resistance mechanisms that tumour cells or neurons will evolve.

CDK9–Cyclin T1 is a member of the cyclin-dependent kinase family, crucial for regulating transcription elongation through phosphorylation of RNA polymerase II, thereby licensing transcriptional elongation of anti-apoptotic and oncogenic genes such as MYC and MCL$^{-1}$. Selective CDK9 inhibition has therefore emerged as a strategy for cancer therapy and for resensitising tumour cells to chemotherapeutics (Table 4). The observed binding mode of compound 4 in the ATP-binding cleft shows a remarkable mimicry of Alvocidib, a well-characterised CDK inhibitor. However, compound 4 not only overlaps spatially with Alvocidib but also forms additional key interactions—including three hydrogen bonds involving catalytic residues such as Glu107 and Asp167. These interactions are vital for inhibitory potency and selectivity. The superior docking score (–8.78 kcal/mol vs –8.18 kcal/mol for Alvocidib) suggests enhanced affinity, which could translate into improved inhibitory efficacy in biological assays.

**Table 4:** Details of Potential Targets, Control Inhibitors, and Functional Roles.

| Target | Pdb code | Control inhibitor | Target role |
|---|---|---|---|
| CDK9/cyclin T1 | 8K5R | Alvocidib | The CDK9–cyclin T1 complex plays a key role in promoting transcriptional elongation by RNA polymerase II, enhancing the expression of oncogenes such as c-Myc and MCL-1. Since transcriptional deregulation—driven in part by MYC amplification—is a hallmark of many cancers, targeting transcriptional cofactors like CDK9 has emerged as a promising therapeutic strategy to suppress aberrant oncogene expression.[28] |
| Caspase-6 | 3OD5 | Emricasan | Caspases, an evolutionarily conserved family of cysteine-dependent proteases, play essential roles in modulating different biological processes, including apoptosis, proliferation and inflammation.<br>A plethora of diseases, such as inflammatory, neurological and metabolic diseases, and cancer, are associated with the poor regulation of caspase-mediated cell death and inflammation.<br>Numerous natural and artificial caspase inhibitors have been identified and developed with the intention for therapeutic use.<br>Due to the poor efficacy or toxic effects, only a few synthetic caspase inhibitors have progressed to clinical trials, but none have achieved approval for clinical use so far.[29] |

ISSN 2616-0684 (Print)
ISSN 2616-0692 (Electronic)

The identification of Caspase 6 as a secondary target is particularly interesting given its role in neuronal apoptosis and neurodegenerative disorders (Table 4). The docking results show that compound 4 occupies the catalytic pocket, interacting with the catalytic dyad (His121 and Cys163) and critical specificity residues like Arg64 and Tyr217. These interactions are consistent with the known caspase-inhibitor mechanisms, and provide a docking score (–8.52 kcal/mol) which approaches that of Emricasan (a clinical-stage pan-caspase inhibitor).

Unlike the ubiquitous executioner caspases, caspase 6 is implicated in axonal pruning, chronic neuroinflammation, and neurodegeneration (Table 4). Active caspase 6 is detectable in early human brain pathology long before overt neuronal loss, making it an attractive disease-modifying target.[26] Yet the active-site similarity across the caspase family has hampered drug discovery, and no caspase-directed therapy has been approved to date; late-stage candidates such as Emricasan ultimately stalled in clinical trials.[2] The identification of compound 4 as a dual CDK9/Caspase 6 inhibitor may offer a noteworthy advancement in the evolving field of kinase and caspase-targeted drug discovery. While several studies have separately explored inhibitors of CDK9 or Caspase 6[30, 31], none to our knowledge have reported a non-covalent dual inhibitor showing strong binding affinity to both enzymes with potential clear selectivity.

Similarly, Caspase-6 has long been a challenging target due to its structural and functional similarity to other caspases such as Caspase-3 and Caspase-7. Many known inhibitors, such as Emricasan, failed to achieve isoform specificity, often acting as wide-spectrum caspase blockers, which contribute to dose-limiting toxicities and discontinuation of clinical trials.[32] Compound 4, however, displayed a favorable interaction with Caspase-6's active site and showed no effective docking poses in Caspase-7 or Caspase-9. This outcome provides a promising step toward the discovery of selective Caspase-6 inhibitors.

*ADME prediction*

The pharmacokinetics analysis of the synthesised molecule (Compound 4) showed that the compound fulfils classical oral drug-likeness criteria. It has a molecular weight of 439 Da, cLogP 0.99, and a topological polar surface area (TPSA) of 132 Å², satisfying all Lipinski, Pfizer, and Golden-Triangle filters (Table 5). Predicted human intestinal absorption was high (HIA = 0.81), and passive permeability was at the threshold of acceptability in Caco-2 (–5.33 log cm $s^{-1}$). Distribution modelling predicted high plasma-protein binding (92 %) and negligible blood–brain-barrier penetration. The compound is estimated to be predominantly metabolised by CYP2C9, with minimal inhibition of major CYP isoforms. The systemic clearance was low (0.56 mL $min^{-1}$ $kg^{-1}$), suggesting moderate exposure, despite having a short half-life prediction.

The *in silico* ADME profile indicates favorable chemical properties and oral availability of the predicted dual inhibitor. The compound 4 showed compliance with the key physicochemical properties (rules of five), a moderate logP (0.99), and an SA score of 3.6, collectively suggesting good lipophilicity and synthetic acceptability. Although the Caco-2 permeability is suboptimal, the high predicted intestinal absorption indicates overall good absorption potential. However, the high score of "< 20 % F", which indicates low oral bioavailability, highlights a necessity for solubility-enhancing strategies such as salts or amorphous dispersions.

In distribution, extensive plasma binding (92 %) may restrict the free fraction available to engage intracellular CDK9/Cyclin T1 or cytosolic Caspase-6, but similar binding behaviour is observed for many marketed kinase and protease inhibitors. Lack of BBB penetration is beneficial since neither therapeutic target is located in the CNS; consequently, peripheral exposure may limit the off-target neurological effects.

Metabolic predictions identified the compound as a CYP2C9 substrate and moderate inhibitor; although this identification may raise concerns regarding potential drug–drug interactions, these risks could be managed through standard DDI screening protocols. Low intrinsic clearance combined with short-estimated half-life implies elimination dominated by metabolism rather than distribution; controlled-release or pro-drug approaches could be explored to sustain low concentrations above the sub-micromolar IC50 values predicted in our docking studies of both enzymes. Considering all data, the ADME profile supports the viability of the compound 4 as an orally active, dual CDK9/Caspase-6 inhibitor. The favorable absorption and manageable metabolic profile align with the therapeutic rationale of simultaneously attenuating transcriptional hyperactivation (via CDK9) and dysregulated apoptosis (via Caspase-6).

**Table 5:** *In silico* ADME profile of the synthesised compound (compound 4).

| Category | Key parameter | Predicted value | Optimal value |
|---|---|---|---|
| Physicochemical & drug-likeness | MW | 439 Da | 100–600 |
| | cLogP / cLogD 7.4 | 0.99 / 0.89 | Optimal 0–3 |
| | TPSA | 132 Å² | ≤ 140 Å² |
| | H-bond donors/acceptors | 1 / 9 | ≤ 5 / ≤ 10 |
| | Rotatable bonds | 5 | ≤ 11 |
| | Lipinski, Pfizer, Golden Triangle | Accepted | – |
| | QED / SA score | 0.47 / 3.60 | QED 0.34–0.67; SA < 6 |
| Absorption | Caco-2 (log cm $s^{-1}$) | –5.33 | > –5.15 desirable |
| | HIA probability | 0.81 | > 0.5 = likely absorbed |
| | F<20 % probability | 0.94 | High value = risk of low oral F |
| Distribution | PPB | 92 % | < 90 % preferred |
| | VD | 1.0 L $kg^{-1}$ | 0.04–20 |
| | BBB penetration prob. | 0.01 | < 0.1 = BBB– |
| Metabolism | CYP liabilities | Substrate: 2C9 (0.96) ≫ 2C19 (0.56) ≈ 3A4 (0.46); weak inhibitor only of 2C9 (0.63) | – |
| Excretion | Clearance | 0.56 mL $min^{-1}$ $kg^{-1}$ | < 5 = low |
| | t½ probability (long) | 0.12 | < 0.5 = short t½ |

## Conclusion

In conclusion, a new derivative of 1,2,3-triazole containing a cyclohexa-2,4-dienone ring combined in the same matrix was synthesised using precedent methodologies. The *in-silico* results suggest that compound 4 is a promising dual inhibitor, with a particularly strong and geometrically optimal fit in CDK9–Cyclin T1 due to its complete coverage of the catalytic residues, a three-point hydrogen-bond network (including the pivotal Asp167), and favourable binding energy relative to Alvocidib.
Finally, these findings offer a strong rationale for further optimisation and experimental validation of compound 4 as a potential dual CDK9/Caspase-6 inhibitor. Further investigations, including molecular dynamics (MD) simulations to confirm binding stability, and in vitro enzyme inhibition assays, are recommended to validate these computational predictions. Additionally, selectivity profiling against closely related CDKs and caspases would be necessary to define its specificity and therapeutic potential.

## Conflict of Interest

The authors declare no conflict of interest.

## Authors' Declaration

The authors hereby declare that the work presented in this article is original and that any liability for claims relating to the content of this article will be borne by them.

## Acknowledgments

The authors would like to thank the Department of Chemistry, College of Science, Al Muthanna University, for providing the facilities used during this work.

## References

1. Manwar H, Al-Shuhaib, Z, Hussein KA. Synthesis and molecular docking studies of new tetrazole-acetamide derivatives as anti-cancer agent. Trop J Nat Prod Res. 2024;8(8):8093–8100.
2. Kumar N, Goel N. Heterocyclic compounds: importance in anticancer drug discovery. Anti-Cancer Agents Med. Chem. 2022;22(19):3196–3207.
3. Mateev E, Georgieva M, Zlatkov A. Pyrrole as an important scaffold of anticancer drugs: recent advances. J Pharm Pharm Sci. 2022; (25):24–40.
4. Damayanti D, Iktiarani A, Gymnastiar A. Analysis of active compounds and *in silico* study of vigna unguiculata as an anti-alzheimer disease agent. Trop J Nat Prod Res. 2025; 9(1):219 -228.
5. Kondeva-Burdina M, Mateev E, Angelov B, Tzankova V, Georgieva M. *In silico* evaluation and *in vitro* determination of neuroprotective and MAO-B inhibitory effects of pyrrole-based hydrazones: A therapeutic approach to Parkinson's disease. Molecules. 2022;27(23):8485.
6. Jeelan N, Basavarajaiah S, Shyamsunder K. Therapeutic potential of pyrrole and pyrrolidine analogs: an update. Mol Divers. 2022;26(5):2915–37. Doi: https://doi.org/10.1007/s11030-022-10387-8.
7. Alghamdi SB, Abdallah WE, Abdelshafeek KA. Assessment of antioxidant, antimicrobial, cytotoxic activities and isolation of some chemical constituents from different extracts of *Pergularia daemia*. Trop J Nat Prod Res. 2021; 5(10):1816-1827.
8. Ding L, Cao J, Lin W, Chen H, Xiong X, Ao H, Cui Q. The roles of cyclin-dependent kinases in cell-cycle progression and therapeutic strategies in human breast cancer. Int J Mol Sci. 2020; 21(6):1960. Doi: https://doi.org/10.3390/ijms21061960.
9. Mandal R, Becker S, Strebhardt K. Targeting CDK9 for anti-cancer therapeutics. Cancers. 2021; 13(9):2181. Doi: https://doi.org/10.3390/cancers13092181.
10. Flores J, Noël A, Fillion ML, LeBlanc AC. Therapeutic potential of Nlrp1 inflammasome, Caspase-1, or Caspase-6 against Alzheimer disease cognitive impairment. Cell Death Differ. 2022; 29(3):657–669.
11. Mazyed H, Nahi R. Synthesis and antioxidant study of new1,3-oxazepin-4,7-dione and1,2,3-triazole derivatives. Int J Pharm Res. 2020; 12(1):252–259.
12. Kozan A, Nahi R. Synthesis And Molecular Docking Studies Of New Pyrimidinone Ring Containing 1,2,3-Triazole Derivatives. Int J Drug Deliv Technol. 2023; 13(3):1005–1010.
13. Kozan A, Nahi R. Combination And Molecular Docking Studies Of 1,2,3-Triazole And Pyrimidin-2-Thione Rings For Potential Anti-COVID-19 Activity. J Heal Soc Sci. 2023; 8(3):249–261.
14. Daina A, Michielin O, Zoete V. SwissTargetPrediction: updated data and new features for efficient prediction of protein targets of small molecules. Nucleic Acids Res. 2019; 47(W1):W357–W364. Doi: https://doi.org/10.1093/nar/gkz382.
15. Allouche A. Software news and updates gabedit—a graphical user interface for computational chemistry softwares. J Comput Chem. 2012; 32:174–182. Doi: https://doi.org/10.1002/jcc.21600.
16. Kotynia A, Marciniak A, Kamysz W, Neubauer D, Krzyżak E. Interaction of positively charged oligopeptides with blood plasma proteins. Int J Mol Sci. 2023; 24(3):2836. Doi: https://doi.org/10.3390/ijms24032836.
17. Trott O, Olson AJ. AutoDock Vina: improving the speed and accuracy of docking with a new scoring function, efficient optimization, and multithreading. J Comput Chem. 2010; 31(2):455–461. Doi: https://doi.org/10.1002/jcc.21334.
18. Biovia, D. Discovery studio modeling environment, release 2017 Dassault Systèmes. San Diego, CA, USA, 2016.
19. Kartika, I, Syach A, Larasati D, Pitaloka S, Octaviany S, Kurniadewi F, Namirah I. *In-silico* molecular docking and admet prediction of natural compounds in oncom. Trop J Nat Prod Res. 2024; 8(10942):6737–6740.
20. CCozza G, Zonta F, Vedove A, Venerando A, Dall'Acqua S, Battistutta R, Lolli G. Biochemical and cellular mechanism of protein kinase CK2 inhibition by deceptive curcumin. FEBS J. 2020; 287(9):1850–1864. Doi: https://doi.org/10.1111/febs.15111
21. Freeman B, Hopkins D, Mikochik J, Vacca P, Gao H, Naylor-Olsen A, Trotter W. Discovery of kb-0742, a potent, selective, orally bioavailable small molecule inhibitor of cdk9 for myc-dependent cancers. J Med Chem. 2023; 66(23):15629–15647.
22. Havran M, Chong C, Childers E, Dollings J, Dietrich A, Harrison L, Robichaud J. 3,4-Dihydropyrimido(1,2-a)indol-10(2H)-ones as potent non-peptidic inhibitors of caspase-3. Bioorg Med Chem. 2009; 17(22):7755–7768. Doi: https://doi.org/10.1016/j.bmc.2009.09.036.
23. Wang J, Cao Q, Liu X, Wang T, Mi W, Zhang Y, Su D. Crystal structures of human caspase 6 reveal a new mechanism for intramolecular cleavage self-activation. EMBO Rep. 2010; 11(11):841–847. Doi: https://doi.org/10.1038/embor.2010.141.
24. Wei Y, Fox T, Chambers P, Sintchak J, Coll T, Golec M, Charifson S. The structures of caspases-1, -3, -7 and -8 reveal the basis for substrate and inhibitor selectivity. Chem Biol. 2000; 7(6):423–432.
25. Van S, Wang D, Medina-Cleghorn D, Lee S, Bryant C, Altobelli C, Renslo R. Engaging a non-catalytic cysteine residue drives potent and selective inhibition of caspase-6. J Am Chem Soc. 2023; 145(18):10015–10021.
26. Graham K, Ehrnhoefer E, Hayden R. Caspase-6 and neurodegeneration. Trends Neurosci. 2011;34(12):646–656.

**ISSN 2616-0684 (Print)**
**ISSN 2616-0692 (Electronic)**

27. Smith E, Soti S, Jones A, Nakagawa A, Xue D, Yin H. Non-steroidal anti-inflammatory drugs are caspase inhibitors. Cell Chem Biol. 2017; 24(3):281–292.
28. Cheng S, Qu Q, Wu, J, Yang J, Liu H, Wang W, Leung H. Inhibition of the CDK9–cyclin T1 protein–protein interaction as a new approach against triple-negative breast cancer. Acta Pharm Sin B. 2022; 12(3):1390–1405. Doi: https://doi.org/10.1016/j.apsb.2021.10.024.
29. Dhani S, Zhao Y, Zhivotovsky B. A long way to go: caspase inhibitors in clinical use. Cell Death Dis. 2021; 12(10):1–13.
30. Mo C, Wei N, Li T, Bhat A, Mohammadi M, Kuang C. CDK9 inhibitors for the treatment of solid tumors. Biochem Pharmacol. 2024; 229:116470. Doi: https://doi.org/10.1016/j.bcp.2024.116470.
31. Tubeleviciute-Aydin A, Beautrait A, Lynham J, Sharma G, Gorelik A, Deny J, LeBlanc C. Identification of Allosteric Inhibitors against Active Caspase-6. Sci Rep. 2019; 9(1):1–19.
32. Eguchi A, Koyama Y, Wree A, Johnson D, Nakamura R, Povero D, Feldstein E. Emricasan, a pan-caspase inhibitor, improves survival and portal hypertension in a murine model of common bile-duct ligation. J Mol Med. 2018; 96(6):575–583.